Semiempirical tight-binding band structures of wurtzite semiconductors: AlN, CdS, CdSe, ZnS, and ZnO

Akiko Kobayashi, Otto F. Sankey, Stephen M. Volz, and John D. Dow
Department of Physics, University of Illinois at Urbana—Champaign, 1110 West Green Street, Urbana, Illinois 61801
(Received 13 September 1982)

Semiempirical tight-binding electronic energy band structures of the following wurtzite materials are reported: AlN, CdS, CdSe, ZnS, and ZnO.

I. INTRODUCTION

Recent studies of the electronic energy levels of substitutional defects,[1] interstitials,[2] and surfaces[3] in zinc-blende semiconductors have demonstrated the advantages of having a parametrization of the host energy bands in terms of a nearest-neighbor empirical tight-binding theory.[4–8] In this paper we produce an sp^3 tight-binding model of the wurtzite semiconductors AlN, CdS, CdSe, ZnS, and ZnO.

II. THEORY

The wurtzite unit cell contains four atoms, two anions, and two cations, as shown in Fig. 1(a). The basis vectors $\vec{t}_1$, $\vec{t}_2$, $\vec{t}_3$, and $\vec{t}_4$ are $(0,0,0)$, $(a/\sqrt{3},0,c/2)$, $(a/\sqrt{3},0,c/8)$, and $(0,0,5c/8)$, where a is the length of a hexagonal side and c is the repeat distance along the z direction. The anions are at $\vec{t}_1$, and $\vec{t}_2$; the cations are at $\vec{t}_3$, and $\vec{t}_4$. The reciprocal lattice, shown in Fig. 1(b), is also hexagonal. The direct lattice vectors are defined as $\vec{a}=((\sqrt{3}/2)a,(-1/2)a,0)$, $\vec{b}=(0,a,0)$, and $\vec{c}=(0,0,c)$, and the reciprocal-lattice vectors are $\vec{b}_a=((4\pi/\sqrt{3})/a,0,0)$, $\vec{b}_b=((2\pi/\sqrt{3})/a,2\pi/a,0)$, and $\vec{b}_c=(0,0,2\pi/c)$.

A. The Hamiltonian

We assume an sp^3 basis centered at each of the four atomic sites per unit cell, (namely, one s orbital and three p orbitals per site), leading to a $16N\times 16N$

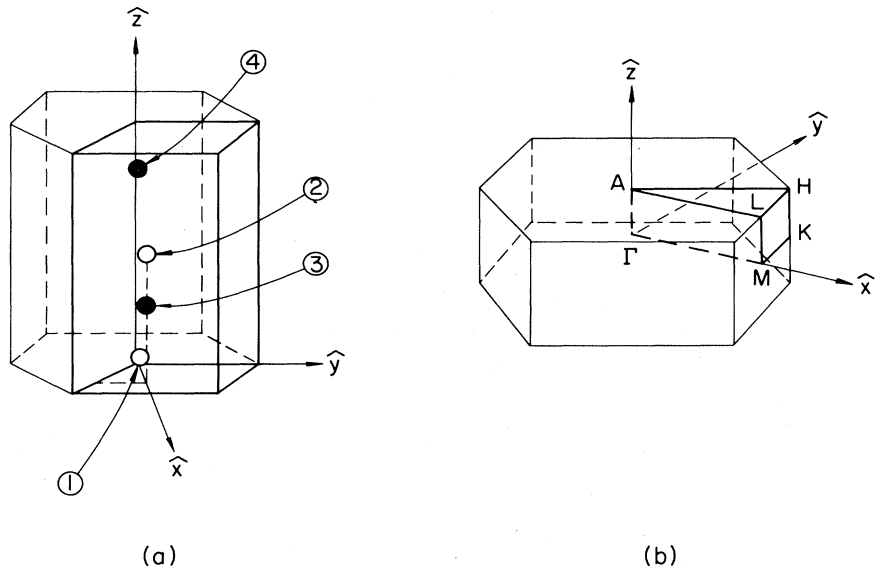

FIG. 1. (a) Hexagonal close-packed structure with four basis atoms, where 1 and 2 are anions, 3 and 4 are cations, with basis vectors $\vec{t}_1=(0,0,0)$, $\vec{t}_2=(a/\sqrt{3},0,c/2)$, $\vec{t}_3=(a/\sqrt{3},0,c/8)$, and $\vec{t}_4=(0,0,5c/8)$, respectively. (b) The reciprocal lattice. The symmetry points of the Brillouin zone are $\Gamma=(0,0,0)$, $K=(2\pi/a)(1/\sqrt{3},\frac{1}{3},0)$, $M=(2\pi/a)(1/\sqrt{3},0,0)$, $A=(2\pi/c)(0,0,\frac{1}{2})$, $H=(2\pi/a)(1/\sqrt{3},\frac{1}{3},a/2c)$, $L=(2\pi/a)(1/\sqrt{3},0,a/2c)$.

 ©1983 The American Physical Society

Hamiltonian, where N is the number of unit cells. We limit the number of nonzero tight-binding parameters to one-center on-site integrals and nearest-neighbor two-center integrals, as discussed by Slater and Koster.[5] We treat the four nearest-neighbor atoms as equivalent, even though the crystal is not cubic (this has a negligible effect on the energy levels of localized perturbations[9]). The small crystal-field splittings which differentiate between the p_z orbital and the p_x and p_y orbitals are neglected (they are due to second-nearest neighbors and more distant neighbors). Thus the model has nine independent parameters: the four on-site matrix elements $E(s,a)$, $E(p,a)$, $E(s,c)$, and $E(p,c)$ (where s and p refer to the basis states, and a and c refer to anion and cation), and five nearest-neighbor transfer matrix elements $V(ss\sigma)$, $V(sp\sigma)$, $V(ps\sigma)$, $V(pp\pi)$, and $V(pp\sigma)$, where the orientation of the p orbitals are denoted by σ and π (see the Appendix), and the first (second) index refers to the anion (cation). In the development that follows, we consider the true C_{3v} symmetry, so that the simplifications can be easily relaxed, if desired.

For each wave vector $\vec{k}$, we construct the following Bloch-type linear combination of localized orbitals

$$|n,b,\vec{k}) = N^{-1/2} \sum_{\vec{R}} \exp[i\vec{k}\cdot(\vec{R}+\vec{t}_b)]\,|n,b,\vec{R}) ,$$

where $|n,b,\vec{R})$ is a localized wave function centered at the site $\vec{R}+\vec{t}_b$ ($b=1$, 2, 3, or 4 for the four atoms in a unit cell [Fig. 1(a)], and $n=s$, p_x, p_y, or p_z). The crystal eigenstates are linear combination of the above Bloch-type basis states,

$$|\vec{k},\lambda\rangle = \sum_{n,b} |n,b,\vec{k})(n,b,\vec{k}\,|\,\vec{k},\lambda\rangle .$$

The corresponding Schrödinger equation in a Bloch-type basis can be written as

$$\sum_{m,b'} [\,(n,b,\vec{k}\,|\,H\,|\,m,b',\vec{k}) - \epsilon(\vec{k},\lambda)\delta_{n,m}\delta_{b,b'}](m,b',\vec{k}\,|\,\vec{k},\lambda\rangle = 0 ,$$

where we have

$$(n,b,\vec{k}\,|\,H\,|\,m,b',\vec{k}) = \sum_{\vec{R}} \exp[i\vec{k}\cdot(\vec{R}+\vec{t}_{b'}-\vec{t}_b)] \times (n,b,\vec{0}\,|\,H\,|\,m,b',\vec{R}) .$$

We have taken the overlaps of localized orbitals centered on different sites to be zero and we will now assume that only the Hamiltonian matrix elements between orbitals centered on the same atom or between nearest-neighbor atoms are nonzero.

In the $|n,b,\vec{k})$ basis, the perfect-crystal Hamiltonian, using the C_{3v} point-group symmetry of each site, is the 16×16 matrix

$$\begin{array}{c|cccc} b\backslash b' & 1 & 2 & 3 & 4 \\ \hline 1 & \underline{E}_a & \underline{0} & \underline{H}_{1,3} & \underline{H}_{1,4} \\ 2 & \underline{0} & \underline{E}_a & \underline{H}_{1,4} & \underline{H}_{2,4} \\ 3 & \underline{H}^{\dagger}_{1,3} & \underline{H}^{\dagger}_{1,4} & \underline{E}_c & \underline{0} \\ 4 & \underline{H}^{\dagger}_{1,4} & \underline{H}^{\dagger}_{2,4} & \underline{0} & \underline{E}_c \end{array} .$$

Each element of this matrix is a 4×4 matrix. The on-site matrix for the anions (atoms 1 and 2) is

TABLE I. Nearest-neighbor tight-binding parameters (in eV) of AlN, CdS, CdSe, ZnS, and ZnO. The off-site matrix elements (U's) are related to the zinc-blende V's of Ref. 6 as follows: $4U(s,s)=V(s,s)$, $(4/3)[U(z,z)+2U(x,x)]=V(x,x)$, $(4/3)[U(z,z)-U(x,x)]=V(x,y)$, $(-4/\sqrt{3})U(s,z)=V(sa,pc)$, $(4/\sqrt{3})U(z,s)=V(pa,sc)$. The relationships among the notation used here for the wurtzite structure (U's and U''s), the zinc-blende notation, and the standard notation for the two-center Slater-Koster (Ref. 5) approximation can be found in the Appendix.

	AlN	CdS	CdSe	ZnS	ZnO
$E(s,a)$	−12.104	−11.133	−10.782	−10.634	−19.046
$E(p,a)$	3.581	1.327	1.309	1.574	4.142
$E(s,c)$	−0.096	2.243	1.682	2.134	1.666
$E(p,c)$	9.419	6.673	6.091	6.626	12.368
$V(s,s)$	−10.735	−2.214	−2.016	−4.904	−6.043
$V(x,x)$	5.808	2.976	2.824	3.229	7.157
$V(x,y)$	8.486	4.512	4.324	5.168	10.578
$V(sa,pc)$	8.092	0.936	1.101	0.357	4.703
$V(pa,sc)$	9.755	4.516	3.988	6.240	8.634

$$\underline{E}_a = \begin{array}{c} \\ (s,1\,| \\ (p_z,1\,| \\ (p_x,1\,| \\ (p_y,1\,| \end{array} \begin{array}{c} \begin{array}{cccc} |s,1) & |p_z,1) & |p_x,1) & |p_y,1) \end{array} \\ \begin{bmatrix} E(s,a) & E(s,p_z,a) & 0 & 0 \\ E(s,p_z,a) & E(p_z,a) & 0 & 0 \\ 0 & 0 & E(p_x,a) & 0 \\ 0 & 0 & 0 & E(p_x,a) \end{bmatrix} \end{array} ,$$

where $E(s,p_z,a)$ is taken to be zero and $E(p_z,a)=E(p_x,a)=E(p,a)$, in the approximation that the local environment is tetrahedral (T_d instead of C_{3v}; see the Appendix).

The on-site matrix $\underline{E}_c$ for cation atoms 3 and 4 is the same in form as the above matrix $\underline{E}_a$, except that c replaces a everywhere.

The off-site matrices are $\underline{H}_{1,4}=g_3(\vec{k})\underline{M}_{1,4}$, $\underline{H}_{2,4}=g_2(\vec{k})\underline{M}_{2,4}$, and $\underline{H}_{1,3}=g_1(\vec{k})\underline{M}_{1,3}$, where we have

TABLE II. Energies of band structures (in eV) at symmetry points.

	ZnO		AlN		CdS		CdSe		ZnS	
Symmetry points	Present	Others	Present	Others	Present	Others	Present	Others	Present	Others
$\Gamma_{6c},\Gamma_{1'c}$	16.51	16.51[a]	13.0	13.0[b,c]	8.0	8.0[d]	7.4	7.4[d]	8.2	8.2[d]
Γ_{3c}	7.39	7.39[a]	8.92	8.92[b,c]	4.5	4.5[d]	3.8	3.8[d]	5.1	5.1[d]
Γ_{1c}	3.30	3.30[a]	6.2	6.2[b,c]	2.6	2.6[d]	2.0	2.0[d]	3.8	3.8[d]
$\Gamma_{6v},\Gamma_{1'v}$	0.0	0.0	0.0	0.0	0.0	0.0	0.0	0.0	0.0	0.0
Γ_{5v}	−1.52	−1.52[a]	−1.22	−1.22[b]	−0.6	−0.6[d]	−0.6	−0.6[d]	−0.8	−0.8[d]
Γ_{3v}	−5.85	−5.85[a]	−7.10	−7.10[b]	−2.7	−2.7[d]	−2.5	−2.5[d]	−3.9	−3.9[d]
Γ_{1v}	−20.68	−20.68[a]	−18.40	−18.40[b]	−11.49	−11.49[e]	−11.1	−11.1	−12.3	−12.3[f]
$L_{1'3'c}$	15.53	12.89[a]	13.53	11.93[b,c]	7.75	7.3[d]	7.10	6.7[d]	8.71	7.0[d]
L_{13c}	9.05	7.78[a]	9.99	7.82[b,c]	5.19	5.2[d]	4.48	4.6[d]	5.80	5.3[d]
L_{13v}	−2.34	−1.70[a]	−1.87	−0.46[b]	−0.93	−0.9[d]	−0.93	−0.7[d]	−1.24	−1.1[d]
L_{24v}	−2.44	−1.70[a]	−1.97	−1.65[b]	−0.98	−0.9[d]	−0.98	−0.7[d]	−1.31	−1.1[d]
$L_{1'3'v}$	−5.78	−4.89[a]	−7.52	−5.34[b]	−2.70	−2.7[d]	−2.48	−2.5[d]	−4.09	−3.9[d]
$A_{1'3'c}$	17.01	14.0[a]								
A_{56c}			13.64	13.36[b,c]	8.31	8.3[d]	7.71	7.7[d]	8.62	8.5[d]
A_{13c}	6.11	6.15[a]	8.13	9.06[b,c]	3.86	4.3[d]	3.20	3.7[d]	4.75	5.3[d]
A_{56v}	−0.79	−0.44[a]	−0.64	−0.69[b]	−0.31	−0.3[d]	−0.31	−0.2[d]	−0.42	−0.3[d]
A_{13v}	−3.63	−4.3[a]	−3.86	−4.12[b]	−1.63	−1.7[d]	−1.53	−1.6[d]	−2.18	−2.3[d]
H_{3c}	9.74	8.3[a]	10.38	9.96[b,c]	5.49	6.4[d]	4.76	5.7[d]	6.04	6.6[d]
H_{3v}	−2.30	−1.48[a]	−1.84	0.15[b]	−0.92	−0.3[d]	−0.92	−0.3[d]	−1.22	−0.8[d]
H_{12v}	−3.13	−2.37[a]	−2.50	−4.47[b]	−1.26	−1.7[d]	−1.26	−1.5[d]	−1.67	−2.3[d]
$H_{3'v}$	−5.82	−4.59[a]	−7.88	−4.54[b]	−2.74	−2.5[d]	−2.50	−2.3[d]	−4.25	−3.3[d]
K_{3c}	10.55	9.29[a]								
K_{2v}	−2.30	−2.10[a]	−1.84	−3.05[b]	−0.92	−1.1[d]	−0.92	−1.1[d]	−1.22	−1.7[d]
K_{3v}	−2.63	−2.10[a]	−2.11	−1.75[b]	−1.05	−1.1[d]	−1.05	−0.9[d]	−1.40	−1.7[d]
K_{1v}	−3.90	−2.74[a]	−3.11	−5.51[b]	−1.58	−2.0[d]	−1.57	−1.7[d]	−2.09	−3.0[d]
$K_{3'v}$	−5.63	−4.30[a]	−7.67	−3.22[b]	−2.66	−2.0[d]	−2.42	−2.1[d]	−4.15	−2.8[d]

[a]Pseudopotential calculation of Ref. 10.
[b]Orthogonalized-plane-wave calculations of Ref. 11.
[c]Optical-absorption data of Ref. 12.
[d]Pseudopotential calculations of Ref. 13.
[e]Orthogonalized-plane-wave calculations of Ref. 14.
[f]Orthogonalized-plane-wave calculations for cubic ZnS of Ref. 15.

$$\underline{M}_{1,4}=\begin{array}{c} \\ (s,1\,| \\ (p_z,1\,| \\ (p_x,1\,| \\ (p_y,1\,| \end{array}\begin{array}{c} \begin{array}{cccc} |s,4) & |p_z,4) & |p_x,4) & |p_y,4) \end{array} \\ \begin{bmatrix} U(s,s) & U(s,z) & 0 & 0 \\ U(z,s) & U(z,z) & 0 & 0 \\ 0 & 0 & U(x,x) & 0 \\ 0 & 0 & 0 & U(x,x) \end{bmatrix} \end{array},$$

$$\underline{M}_{2,4}=\begin{array}{c} \\ (s,2\,| \\ (p_z,2\,| \\ (p_x,2\,| \\ (p_y,2\,| \end{array}\begin{array}{c} \begin{array}{cccc} |s,4) & |p_z,4) & |p_x,4) & |p_y,4) \end{array} \\ \begin{bmatrix} f_0^*U'(s,s) & f_0^*U'(s,z) & -f_1^*U'(s,x) & (-\sqrt{3}/2)f_-^*U'(s,x) \\ f_0^*U'(z,s) & f_0^*U'(z,z) & -f_1^*U'(z,x) & (-\sqrt{3}/2)f_-^*U'(z,x) \\ -f_1^*U'(x,s) & -f_1^*U'(x,z) & f_1^*U'(x,x) & (-\sqrt{3}/4)f_-^*[U'(x,x)-U'(y,y)] \\ & & +(3/4)f_+^*[U'(x,x)+U'(y,y)] & \\ (-\sqrt{3}/2)f_-^*U'(x,s) & (-\sqrt{3}/2)f_-^*U'(x,z) & (-\sqrt{3}/4)f_-^*[U'(x,x)-U'(y,y)] & f_1^*U'(y,y) \\ & & & +(3/4)f_+^*[U'(x,x)+U'(y,y)] \end{bmatrix} \end{array},$$

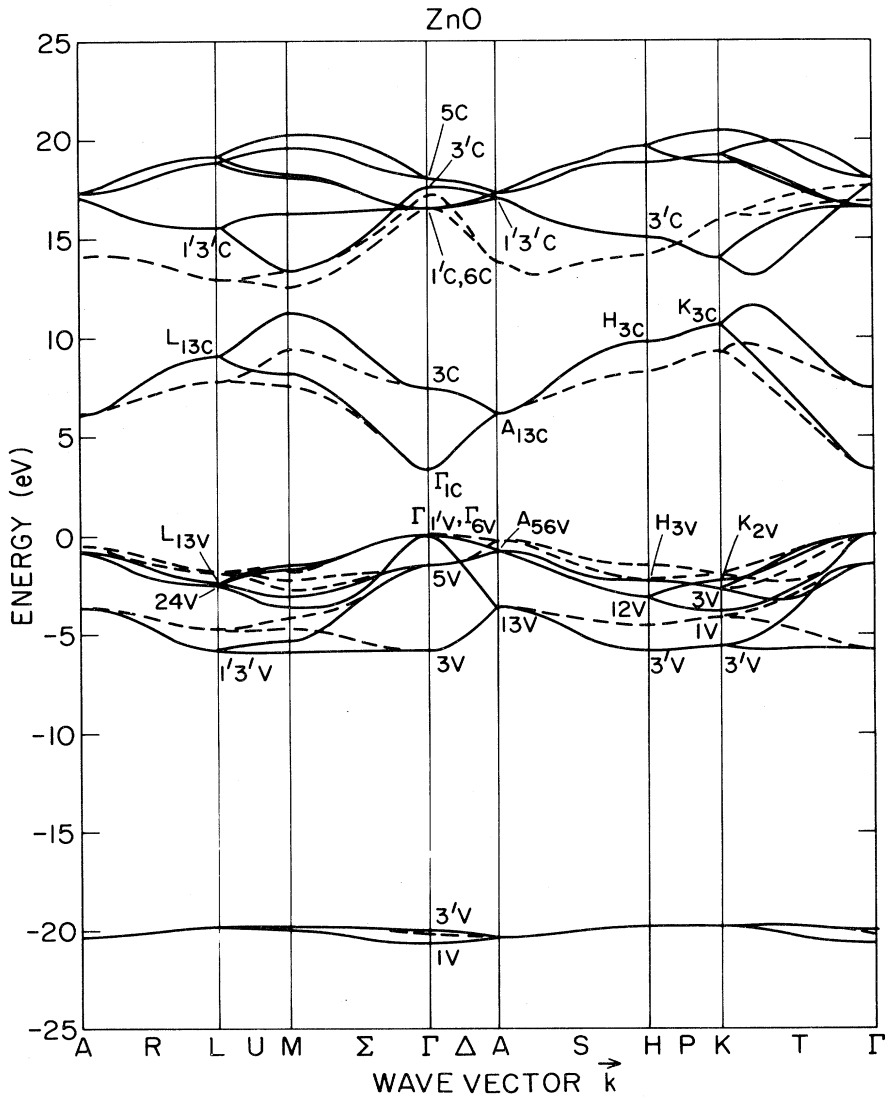

FIG. 2. Band structure of ZnO in the present tight-binding model (solid lines) compared with pseudopotential band structure (dashed lines) of Ref. 10.

$$
\underline{M}_{1,3}=
\begin{array}{c}
\\
(s,1|\\
(p_z,1|\\
(p_x,1|\\
(p_y,1|
\end{array}
\begin{array}{c}
\begin{array}{cccc}
|s,3) & |p_z,3) & |p_x,3) & |p_y,3)
\end{array}\\
\begin{pmatrix}
f_0U'(s,s) & f_0U'(s,z) & f_1U'(s,x) & (\sqrt{3}/2)f_-U'(s,x)\\
f_0U'(z,s) & f_0U'(z,z) & f_1U'(z,x) & (\sqrt{3}/2)f_-U'(z,x)\\
f_1U'(x,s) & f_1U'(x,z) & f_1U'(x,x)+(3/4)f_+[U'(x,x)+U'(y,y)] & (-\sqrt{3}/4)f_-[U'(x,x)-U'(y,y)]\\
(\sqrt{3}/2)f_-U'(x,s) & (\sqrt{3}/2)f_-U'(x,z) & (-\sqrt{3}/4)f_-[U'(x,x)-U'(y,y)] & f_1U'(y,y)+(3/4)f_+[U'(x,x)+U'(y,y)]
\end{pmatrix}
\end{array}
,
$$

and

$$g_1(\vec{k})=\exp[i(-k_1/3+k_2/3+k_3/8)]\,,$$
$$g_2(\vec{k})=\exp[i(k_1/3-k_2/3+k_3/8)]\,,$$
$$g_3(\vec{k})=\exp(-i3k_3/8)\,,$$

$$f_0(\vec{k})=\exp(ik_1)+1+\exp(-ik_2)\,,$$
$$f_1(\vec{k})=\exp(ik_1)-\tfrac{1}{2}-(\tfrac{1}{2})\exp(-ik_2)\,,$$
$$f_+(\vec{k})=1+\exp(-ik_2)\,,$$

and

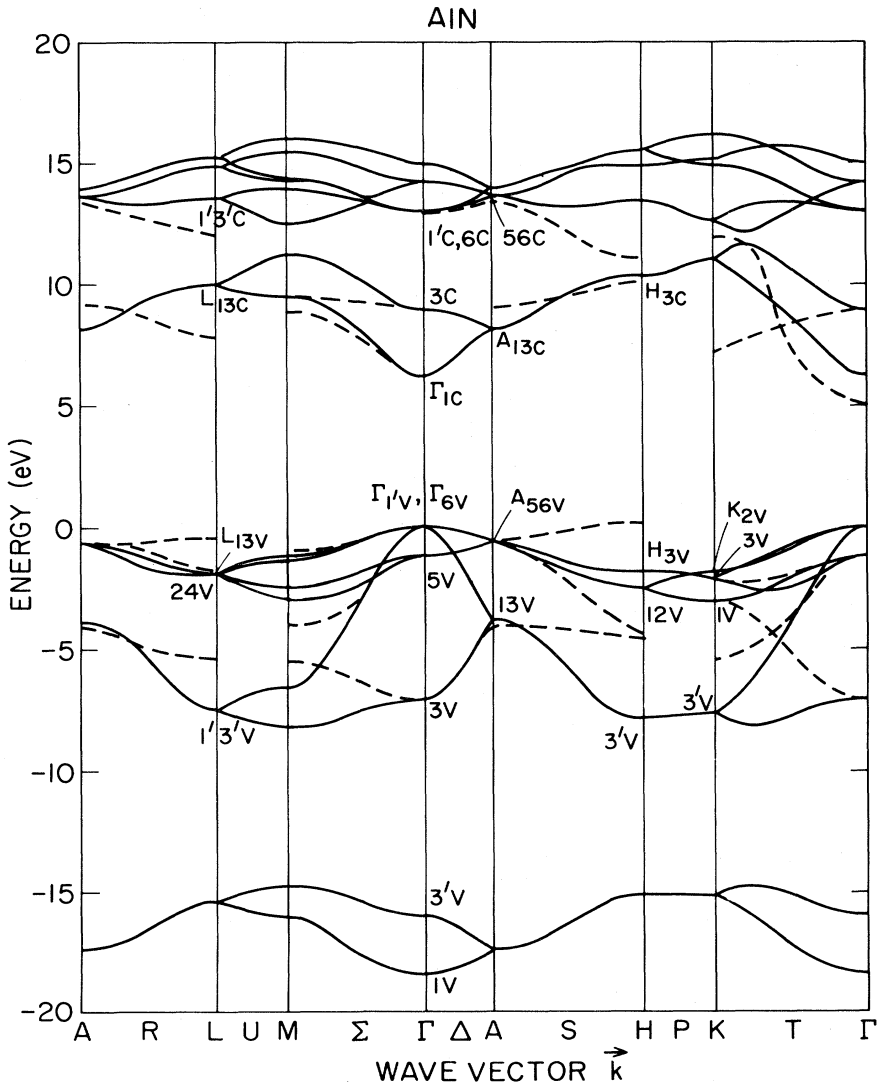

FIG. 3. Band structure of AlN in the present tight-binding model (solid lines) compared with orthgonalized-plane-wave (OPW) band structure (dashed lines) of Ref. 11 with the band gap corrected in accord with that determined by optical absorption (Ref. 12).

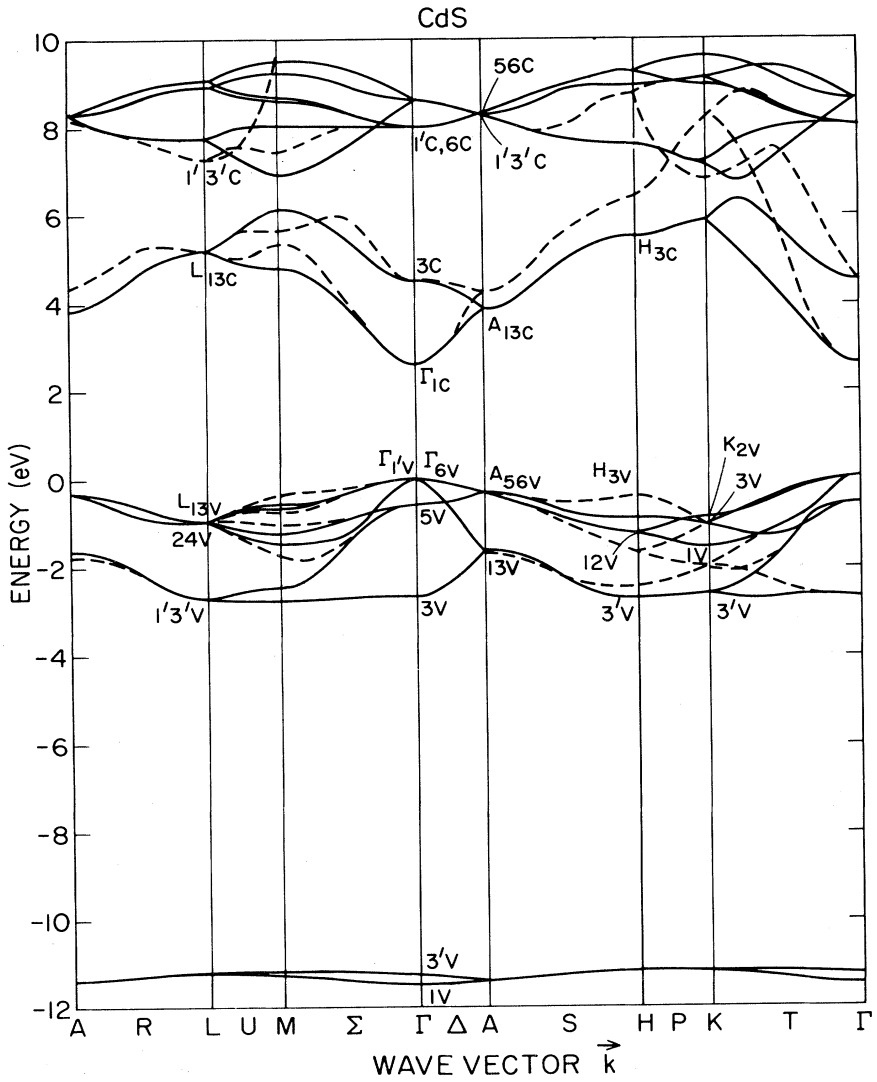

FIG. 4. Band structure of CdS in the present tight-binding model (solid lines) compared with pseudopotential band structure (dashed lines) of Ref. 13.

$$f_{-}(\vec{k})=1-\exp(-ik_2)\ .$$

Here we have $\vec{k}=k_1\vec{b}_1+k_2\vec{b}_2+k_3\vec{b}_3$; $\vec{b}_1$, $\vec{b}_2$, and $\vec{b}_3$ are the reciprocal-lattice vectors divided by 2π, namely, $((2/\sqrt{3})/a,0,0)$, $((1/\sqrt{3})/a,1/a,0)$, and $(0,0,1/c)$, respectively.

The parameters used above are matrix elements of H between localized orbitals $|n,b,\vec{R})$. For example, we have

$$E(s,a)=(s,1,\vec{R}\,|\,H\,|\,s,1,\vec{R})$$
$$=(s,2,\vec{R}\,|\,H\,|\,s,2,\vec{R})\ ,$$

$$E(s,p_z,c)=(s,3,\vec{R}\,|\,H\,|\,p_z,3,\vec{R})$$
$$=(s,4,\vec{R}\,|\,H\,|\,p_z,4,\vec{R})\ ,$$

$$U(x,x)=(p_x,1,\vec{R}\,|\,H\,|\,p_x,4,(\vec{R}-\vec{c}\,))\ ,$$

and

$$U'(z,z)=(p_z,1,\vec{R}\,|\,H\,|\,p_z,3,\vec{R})\ .$$

Following Vogl *et al.*[6] we take the difference between the anion and cation s and p on-site matrix elements of the Hamiltonian to be proportional to the difference in neutral free-atom Hartree-Fock or-

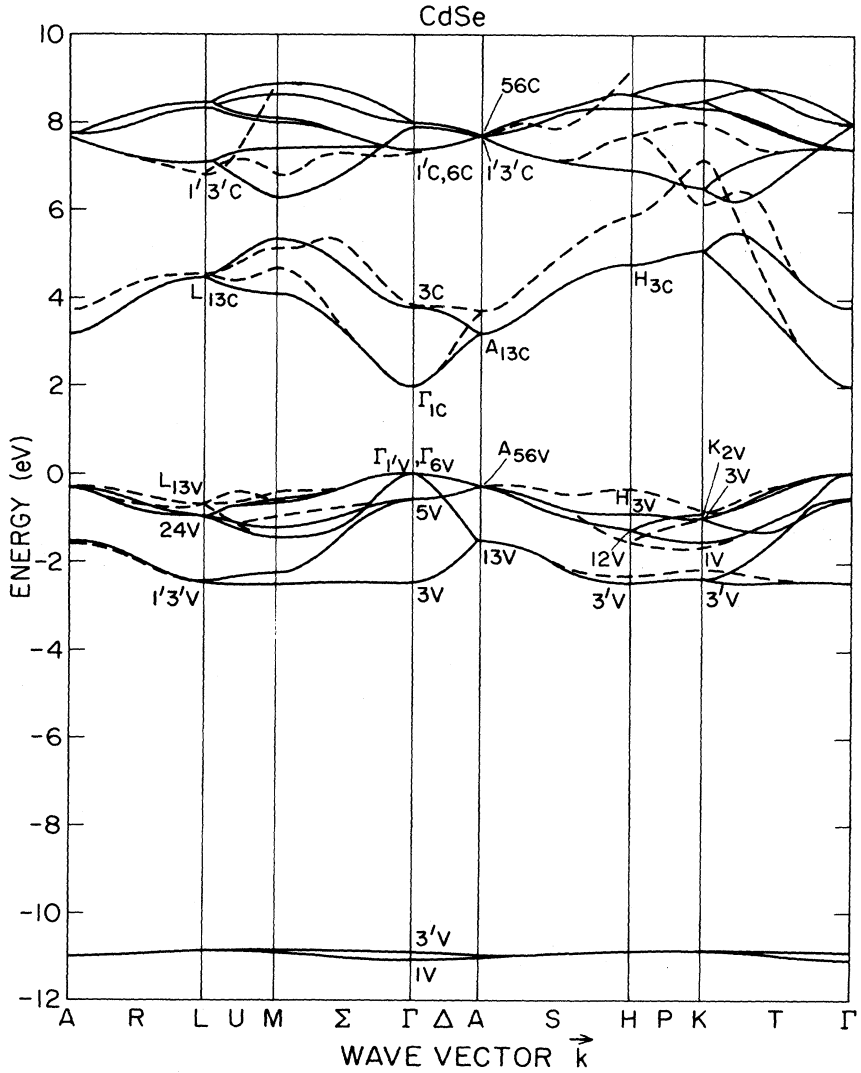

FIG. 5. Band structure of CdSe in the present tight-binding model (solid lines) compared with pseudopotential band structure (dashed lines) of Ref. 13.

bital energies $w(s,a)$, $w(s,c)$, $w(p,a)$, and $w(p,c)$:

$$E(s,a)-E(s,c)=\beta_s[w(s,a)-w(s,c)]$$

and

$$E(p,a)-E(p,c)=\beta_p[w(p,a)-w(p,c)]\ ,$$

where $w(s,a)$, $w(s,c)$, $w(p,a)$, and $w(p,c)$ can be obtained from atomic energy tables.[6] The s (p) proportionality constant, $\beta_s=0.8$ ($\beta_p=0.6$), of Vogl *et al.* is also used here and found to give nearly the best fit to the band structures.

B. The matrix elements

The matrix elements of the Hamiltonian are obtained empirically by fitting to band-structure calculations and available data.[10–15] The band structures are fitted at only the Γ points ($\vec{k}=\vec{0}$), which correspond roughly to fitting the Γ and L points of the zinc-blende band structure; Birman has shown that these points roughly map into one another in materials undergoing zinc-blende–wurtzite phase transitions.[16] Thus by fitting known band structures at $\vec{k}=\vec{0}$ (while paying attention to chemical trends in

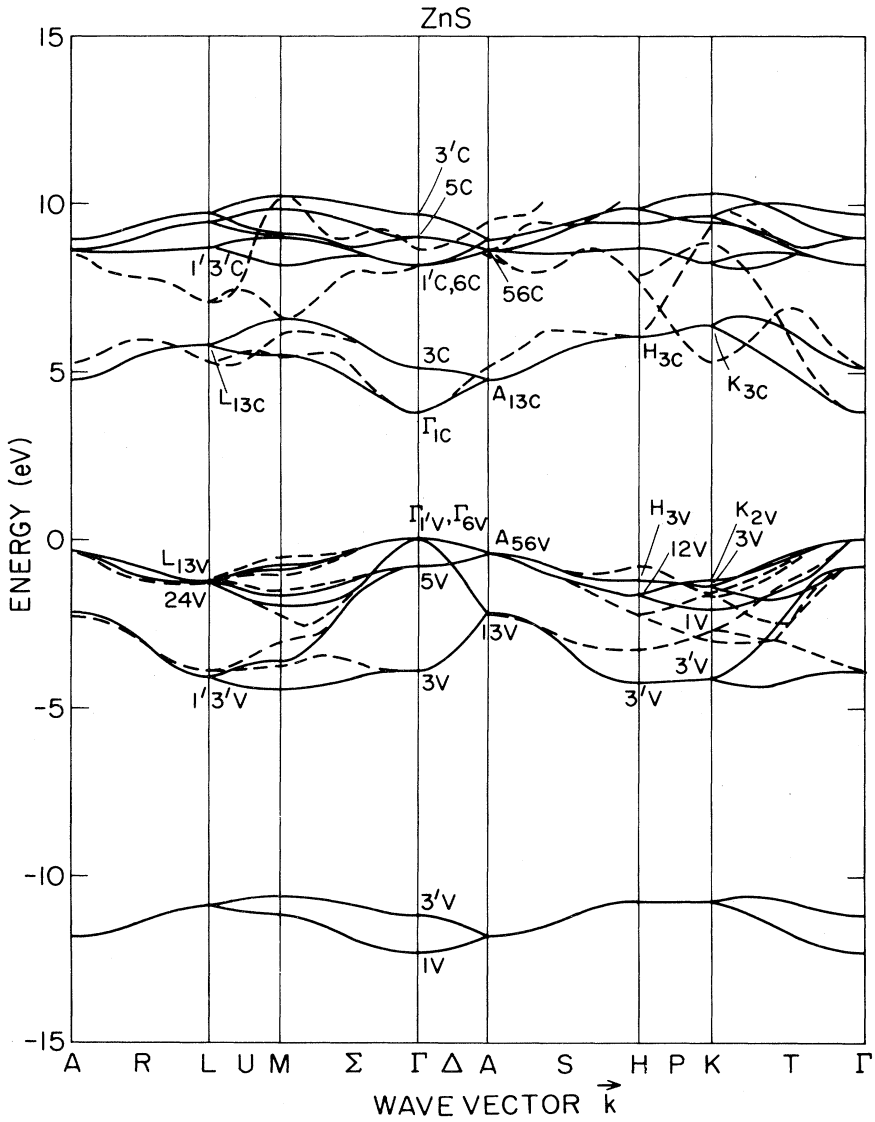

FIG. 6. Band structure of ZnS in the present tight-binding model (solid lines) compared with pseudopotential band structure (dashed lines) of Ref. 13.

the parameters) we have determined the tight-binding parameters of Table I. Hence the Hamiltonian H of the host is completely determined. The band-structure energies at high-symmetry points are listed in Table II, where the present tight-binding fit is compared with previously reported band structures.

Figure 2 shows the ZnO tight-binding band structure obtained by our fitting procedure, in comparison with Chelikowsky's pseudopotential band structure (Ref. 10). As in nearly all tight-binding models, the valence bands are reproduced quite accurately. The narrow lowest valence band near -20 eV corresponds to an atomiclike oxygen $2s$ state, and the upper valence bands are mainly derived from the oxygen $2p$ state with a sizable mixture of Zn $4s$ and $4p$ states. The lowest conduction band is also well reproduced and is composed primarily of the Zn $4s$ state. The uppermost conduction bands are primarily of Zn $4p$ character and are the least accurately reproduced. Fortunately these are also the least important bands in problems concerning the electronic energy levels of defects or other localized perturbations. (The most likely levels to lie in the gap are

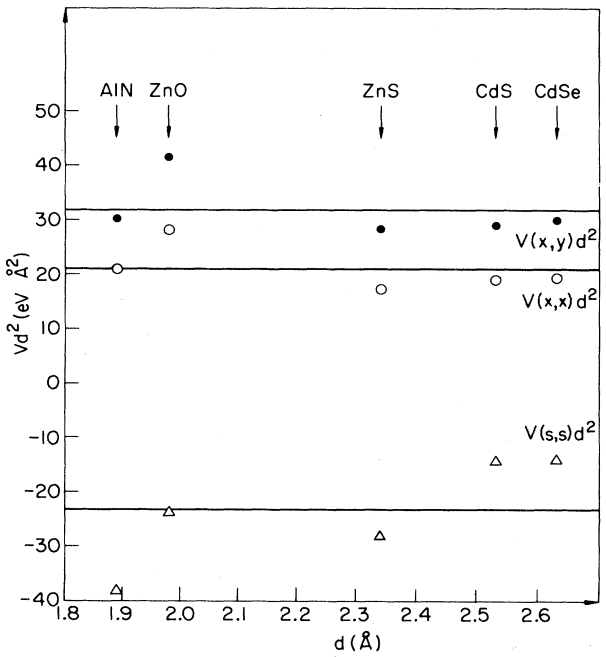

FIG. 7. Interatomic matrix elements $V(s,s)$ (open triangles), $V(x,x)$ (open circles), and $V(x,y)$ (full circles) of Table I (in eV) multiplied by the square of the bond length vs the bond length d (in Å), where the zinc-blende notation (V's here) is related to the wurtzite notation (U's and U''s) as in Table III. Average values are denoted by solid straight lines.

the cation s-like levels pulled down from the lowest conduction band or the anion p-like levels pushed up from the upper valence bands.) Corresponding results hold for AlN, CdS, CdSe, and ZnS. (See Figs. 3–6.)

C. Chemical trends

Empirical tight-binding Hamiltonians such as this are especially useful if their matrix elements exhibit manifest chemical trends. In the present model, the differences of diagonal matrix elements are required to satisfy the rule deduced by Vogl *et al.*[6] for zinc-blende semiconductors: that they be proportional to the corresponding differences in atomic orbital energies,

$$E(l,a)-E(l,c)=\beta_l[w(l,a)-w(l,c)]\ ,$$

where l specifies s or p orbitals.

The remaining off-diagonal matrix elements U and U' are then expected to be nearly independent of the chemical elements in the semiconductor and to scale with bond length d according to Harrison's d^{-2} rule,[17] $U\propto d^{-2}$. The expected scaling is indeed found for the principal matrix elements (Fig. 7).

III. CONCLUSION

The parametrization of the bands of these wurtzite semiconductors provide an accurate representa-

TABLE III. Relationships among parameters of the present model, zinc-blende notation (Ref. 6), and two-center Slater-Koster notation (Ref. 5).

Wurtzite	Zinc blende	Two-center Slater-Koster approximation
$4U(s,s)$	$V(s,s)$	$4V(ss\sigma)$
$(\frac{4}{3})[U(z,z)+2U(x,x)]$	$V(x,x)$	$(4/3)(V(pp\sigma)+2V(pp\pi))$
$(\frac{4}{3})[U(z,z)-U(x,x)]$	$V(x,y)$	$(4/3)(V(pp\sigma)-V(pp\pi))$
$(-4/\sqrt{3})U(s,z)$	$V(sa,pc)$	$(4/\sqrt{3})V(sp\sigma)$
$(4/\sqrt{3})U(z,s)$	$V(pa,sc)$	$(4/\sqrt{3})V(ps\sigma)$
$U'(s,s)-U(s,s)$	0	0
$(\frac{1}{3})[U'(x,x)+U'(y,y)+U'(z,z)]$ $-(\frac{1}{3})[2U(x,x)+U(z,z)]$	0	0
$(\frac{1}{2})[U'(x,x)+U'(y,y)-2U'(z,z)]$ $-(\frac{1}{3})[U(z,z)-U(x,x)]$	0	0
$(\frac{3}{8}[U'(x,x)-U'(y,y)]$ $-(\frac{1}{3})[U(z,z)-U(x,x)]$	0	0
$\sqrt{3}U'(s,z)+(1/\sqrt{3})U(s,z)$	0	0

TABLE III. (*Continued.*)

Wurtzite	Zinc blende	Two-center Slater-Koster approximation
$-\sqrt{3}U'(z,s)-(1/\sqrt{3})U(z,s)$	0	0
$(\sqrt{6}/4)U'(s,x)+(1/\sqrt{3})U(s,z)$	0	0
$(-\sqrt{6}/4)U'(x,s)-(1/\sqrt{3})U(z,s)$	0	0
$(3\sqrt{2}/4)\,U'(z,x)$ $-(\frac{1}{3})[U(z,z)-U(x,x)]$	0	0
$(3\sqrt{2}/4)\,U'(x,z)$ $-(\frac{1}{3})[U(z,z)-U(x,x)]$	0	0

tion of the valence bands and an adequate description of the lowest and most important conduction band. The fact that the matrix elements exhibit trends makes the empirical tight-binding Hamiltonian especially useful for theories of localized perturbations in wurtzites. Soon we shall be reporting studies of deep impurity levels[9] and surface states based on this empirical tight-binding theory.

ACKNOWLEDGMENTS

We gratefully acknowledge stimulating conversations with H. P. Hjalmarson and the support of the Office of Naval Research (Contract No. N00014-77-C-0537) and the U. S. Army Research Office (Contract No. ARO-DAAG29-81-K-0068). The research of S. M. V. was supported by the U. S. Department of Energy, Division of Materials Science (Contract No. DE-AC02-76-ERO1198).

APPENDIX: NOTATION

In this work we neglect the small crystal-field splittings which differentiate between the p_z orbital and p_x and p_y orbitals; hence the local symmetry is taken to be tetrahedral (T_d) rather than C_{3v}, and the on-site matrix elements can be simplified as follows:

$$E(s,p_z,a)=0,\quad E(s,p_z,c)=0\ ,$$

$$E(p_x,a)=E(p_z,a)=E(p,a)\ ,$$

and

$$E(p_x,c)=E(p_z,c)=E(p,c)\ .$$

Furthermore, applying the approximation that the environment is locally tetrahedral (two-center approximation[5]) to the off-diagonal matrix elements corresponds to treating the four nearest-neighbor atoms as equivalent; therefore, the U's in $\underline{H}_{1,4}$ and the U''s in $\underline{H}_{2,4}$ and $\underline{H}_{1,3}$ are not independent. The relationships among the off-diagonal matrix elements of wurtzite (U's and U''s), those of zinc blende,[6] and the standard notation of Slater and Koster[5] are given in Table III.

[1]H. P. Hjalmarson, P. Vogl, D. J. Wolford, and J. D. Dow, Phys. Rev. Lett. 44, 810 (1980); H. P. Hjalmarson, Ph.D. thesis, University of Illinois, 1979 (unpublished).

[2]O. F. Sankey and J. D. Dow, Phys. Rev. B 27, 7641 (1983).

[3]R. E. Allen and J. D. Dow, J. Vac. Sci. Technol. 19, 383 (1981).

[4]D. J. Chadi, Phys. Rev. B 16, 790 (1977).

[5]J. C. Slater and G. F. Koster, Phys. Rev. 94, 1498 (1954).

[6]P. Vogl, H. P. Hjalmarson, and J. D. Dow, J. Phys. Chem. Solids (in press).

[7]D. W. Bullet, J. Phys. C 8, 2695, 2705 (1975); in *Solid State Physics,* edited by H. Ehrenreich, F. Seitz, and D. Turnbull (Academic, New York, 1980), Vol. 35, p. 129.

[8]D. H. Lee and J. D. Joannopoulos, J. Vac. Sci. Technol. 17, 987 (1980).

[9]A. Kobayashi, O. F. Sankey, and J. D. Dow, Phys. Rev. B (in press).

[10]J. R. Chelikowsky, Solid State Commun. 22, 351 (1977).

[11]B. Hejda and K. Hauptmanova, Phys. Status Solidi 36, K95 (1969).

[12]P. B. Perry and R. F. Rutz, Appl. Phys. Lett. 33, 319 (1978).
[13]T. K. Bergstresser and M. L. Cohen, Phys. Rev. 164, 1069 (1967).
[14]R. N. Euwema, J. C. Collins, and J. S. Dewitt, Phys. Rev. 162, 710 (1967).
[15]O. V. Farberovich, S. I. Kurganski and E. P. Domashevskaya, Phys. Status Solidi B 97, 631 (1980).
[16]J. L. Birman, Phys. Rev. 115, 1493 (1959).
[17]W. A. Harrison, Phys. Rev. B 16, 790 (1977).